

Realization of linear magnetoelectric effect in the Dirac magnon system Cu_3TeO_6

Yongsen Tang,^{1,*} Lin Lin^{2,3,†}, Guanzhong Zhou,² Wenjing Zhai,² Lin Huang², Junhu Zhang,² Shuhan Zheng,⁴ Meifeng Liu,⁴ Zhibo Yan,² Xiangping Jiang,⁵ Xing'ao Li,¹ and Jun-Ming Liu²

¹*School of Science, Nanjing University of Posts and Telecommunications, Nanjing 210023, China*

²*Laboratory of Solid State Microstructures, Nanjing University, Nanjing 210093, China*

³*Department of Applied Physics, College of Science, Nanjing Forestry University, Nanjing 210037, China*

⁴*Institute for Advanced Materials, Hubei Normal University, Huangshi 435002, China*

⁵*School of Materials Science and Engineering, Jingdezhen Ceramic Institute, Jingdezhen 333403, China*



(Received 3 December 2022; revised 21 April 2023; accepted 31 May 2023; published 12 June 2023)

The three-dimensional antiferromagnet Cu_3TeO_6 has recently drawn significant attention due to the coexistence of Dirac and triply degenerated magnons. Herein, we report that Cu_3TeO_6 , with cubic symmetry, exhibits novel spin-driven ferroelectric polarization (P) with a strong linear magnetoelectric (ME) coupling effect by comprehensive measurements in magnetization and electric polarization. The magnetic field (H)-induced polarization along x -, y -, and z -axes emerges below $T_N \sim 61$ K, indicative of intrinsic coupling between magnetism and ferroelectricity in this cubic lattice. Our results reveal nine nonvanished components of a ME tensor, while only the P_x ($H//z$), P_y ($H//x$), and P_z ($H//y$) components display a remarkable linear response to H . In particular, we observe six ME states—namely, $(\pm P_x, \pm M_z)$, $(\pm P_y, \pm M_x)$, and $(\pm P_z, \pm M_y)$ —that can be generated by applying an external magnetic field in a specific direction, and thus makes Cu_3TeO_6 a very appealing prototype in multifunctional applications. Our results point toward Cu_3TeO_6 as a new, linear ME material and may pave a way to exploring the rich ME response in the presence of a Dirac magnon in a highly symmetric crystal structure.

DOI: [10.1103/PhysRevB.107.214416](https://doi.org/10.1103/PhysRevB.107.214416)

I. INTRODUCTION

The magnetoelectric (ME) effect exhibiting the induction of magnetization (M) by an electric field (E) or electric polarization (P) by a magnetic field (H) has been of extensive concern in recent years due to its wide coverage in condensed matter physics and potential applications for low-power-consumption sensors [1–5]. In principle, the ME effect can be predicted by magnetic point group analysis, available in those materials that allow simultaneously broken time reversal and space inversion symmetries. For instance, in the so-called type-II multiferroics, the specific magnetic order can break the space inversion symmetry and thus couple with the ferroelectric order, although a single magnetic moment only breaks the time reversal symmetry, as exemplified by $\text{Ca}_3\text{CoMnO}_6$ [6], orthorhombic TbMnO_3 and TbMn_2O_5 [7,8], $\text{CaMn}_7\text{O}_{12}$ [9], $M_2\text{Mo}_3\text{O}_8$ (M : $3d$ transition metal) [10,11], and hexagonal ferrites [12]. In addition to these ME multiferroics, few ME materials with a cubic structure of high symmetry, e.g., $\text{LaMn}_3\text{Cr}_4\text{O}_{12}$ and Cu_2OSeO_3 , have also been reported to exhibit a ME effect [13,14]. Noting that the cubic lattice with an inversion center is unfavorable for ferroelectricity by most of us consideration. Nevertheless, recently, more studies have clearly presented that the ferroelectricity may also rise in a cubic lattice of high structural symmetry by considering a perfect match between magnetic and lattice structures, which are highly required for the linear ME effect in centrosymmetric crystals [15]. Clearly, this approach pro-

vides a sound platform for people to explore the new materials with ME coupling and more accurate physical mechanisms of the ME effect.

It is known that various crystal symmetries and low-energy excitations can give rise to an exotic coupling between electricity and magnetism [16]. Among them, the emergence of a nontrivial magnetic structure in chiral magnets hosting a noncollinear incommensurate structure can generate a ME effect due to the broken space inversion symmetry [1,17]. One typical example is the chiral magnet Cu_2OSeO_3 , with its cubic crystal structure, which reveals magnetically driven ferroelectricity in the skyrmion phase and promises to be a building block for the next generation of magnetic storage devices [18,19]. Hence, the hybridization of magnetism and topology is expected to host distinctive ME responses and emergent phenomena [20]. Until recently, an emergent quantum spin excitation called a topological magnon was experimentally realized in the three-dimensional chiral magnet Cu_3TeO_6 [21,22]. A natural question to ask is whether it is possible to realize a ME effect considering the cubic crystal structure with the $Ia-3$ space group.

Structurally, six Cu^{2+} ions form an almost coplanar chiral hexagon, and each ion is vertex-shared by two hexagons, constituting a three-dimensional spin-web structure, as shown in Fig. 1(a). Second, Cu_3TeO_6 hosting a magnetic point group $-3'$ develops a collinear antiferromagnetic (AFM) order along the [111] direction below Néel temperature $T_N \sim 61$ K [23], as illustrated in Figs. 1(a) and 1(b). Obviously, each up-spin relating to a down-spin by central inversion is described as PT symmetry, where P and T are the space inversion and time reversal operations, respectively. There is no spontaneous polarization and net magnetization with the $-3'$ magnetic point

*tangys@njupt.edu.cn

†llin@njfu.edu.cn

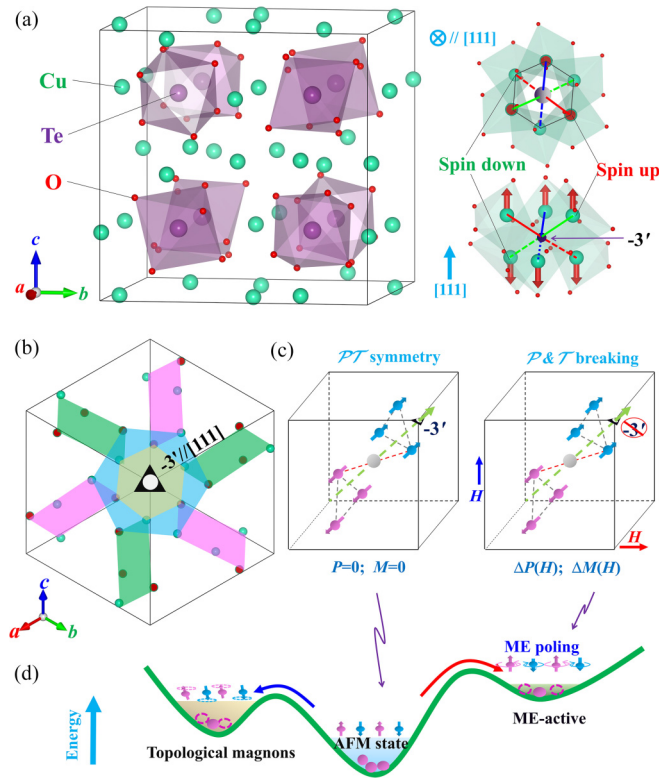


FIG. 1. (a) Schematic crystal and magnetic structures of Cu_3TeO_6 . Each up-spin relates to a down-spin by a central inversion ($-1'$). (b) Illustration of the crystal structure along the $[111]$ direction. (c) Schematic diagram of a spin configuration with a $-3'$ magnetic point group in the absence of a magnetic field, where P and T are space inversion and time reversal operations, respectively. A net electric polarization and magnetization can be generated under the external magnetic field. (d) Schematic illustration of the free-energy landscape for the AFM state, topological magnon state, and ME-active state.

group in the ground state. However, a ME state can be obtained upon symmetry breaking by applying a magnetic field parallel or perpendicular to magnetic moments, as shown in Fig. 1(c), according to symmetry-operational similarity (SOS) theory [16]. Therefore, an experimental detection of a ME effect in Cu_3TeO_6 plays an important role in understanding the magnetically induced ferroelectricity in conjunction with the topological phase, as schematically shown in Fig. 1(d). In this regard, it is possible to acquire a ME active state with a several-millielectron volt energy barrier through an appropriate ME pooling procedure, where the space inversion (P) and time reversal (T) operations are simultaneously broken under H stimulation. As discussed in Ref. [21], opening a gap in the triply degenerate Dirac point under an external H may create an effect on the topological spin excitations with a PT symmetry state. Hence, the study of the ME effect may provide an experimental basis for people to discuss the changes of topological spin excitations and the symmetry. Our work gives an affirmative answer that a linear ME effect can be realized in this high-symmetric Dirac magnon system Cu_3TeO_6 .

In this work, we systematically investigate the magnetic property and ME response in Cu_3TeO_6 single crystals. The

magnetically induced electric polarization (P) along the x , y , and z -axes emerges below $T_N \sim 61$ K, indicative of intrinsic coupling between magnetism and ferroelectricity in this cubic lattice. The anisotropic ME effect is also unambiguously demonstrated, whereas only three main components display an obviously linear ME response while the other cases among the nine ME tensors exhibit only weak ME states. This consequence will be discussed based on the magnetic point group analysis, and, given the magnetic point group $-3'// [111]$, the linear ME coupling coefficients $\alpha_{xz} = \alpha_{yx} = \alpha_{zy}$ can be established by the symmetry-adapted form of the ME tensor, which is consistent with our experimental observations. Our results thus point toward Cu_3TeO_6 as a new linear ME compound and, more importantly, it may pave a way to exploring the rich ME response in a highly symmetric crystal structure in the presence of Dirac magnons.

II. EXPERIMENTAL DETAILS

Single crystals of Cu_3TeO_6 with a nominal composition were grown from the PbCl_2 flux in the air, following the procedure reported earlier [24]. The crystalline phases of as-grown crystals were checked by x-ray diffraction (XRD) (D8 ADVANCE, Bruker) with a $\text{Cu } K_\alpha$ source ($\lambda = 1.5406 \text{ \AA}$). The back-reflection Laue detector (MWL120, Multiwire Laboratories, Ltd.) was used to check the quality of crystals and determine the crystallographic orientation. The chemical composition was analyzed by electron dispersion spectroscopy (EDS) along with scanning electron microscopy (Quanta 200, FEI).

For magnetic and electrical measurements, the single crystals were cut into three slices with the surface normal to the $[100]$ (x -axis), $[010]$ (y -axis), and $[001]$ (z -axis) directions, respectively. The temperature (T) dependence of magnetic susceptibility (χ) was measured using the Quantum Design Superconducting Quantum Interference Device magnetometer from $T = 10$ to 300 K under the zero-field-cooling (ZFC) and field-cooling (FC) modes, with a cooling magnetic field of $H = 0.1$ T applied along the three directions. Simultaneously, M as a function of H was measured at selected T along different directions.

It is noted that a ME annealing procedure was required before acquiring the pyroelectric current (I) and magnetoelectric current (I_{ME}) measurements. For $+H$ and $\pm E$ annealing conditions, where E is the electric field, the sample was pooled under $\pm E = 180 \text{ kV/m}$ ($//P$) and $+H = 9 \text{ T}$ ($//P$ or $\perp P$) from $T = 100$ K down to a selected T . Then, the ME pooling fields were removed and there was a half-hour wait, after which the current was collected by sweeping T or H using a Keithley 6517A electrometer equipped in the Physical Property Measurement System (Quantum Design). The electric polarization P as a function of $T(H)$ was calculated by integrating the pyroelectric current (or magnetoelectric current) with time in the standard procedure [25].

III. RESULTS AND DISCUSSION

A. Structural characterization

The crystal structure of Cu_3TeO_6 was checked by performing the XRD measurements at room temperature. First,

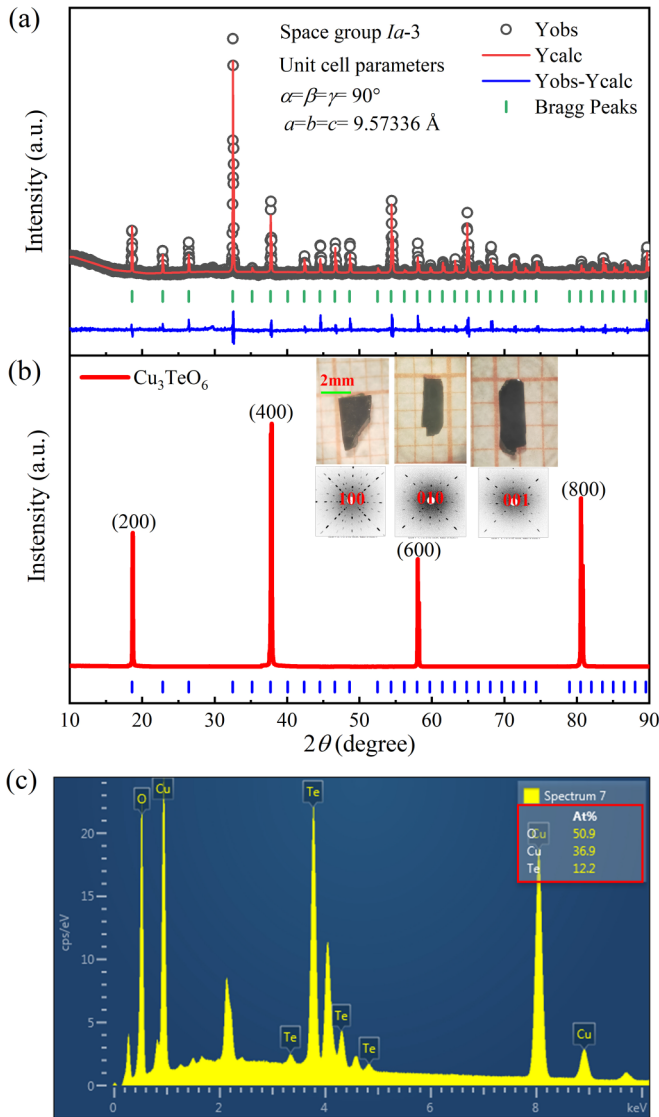


FIG. 2. (a) The refined XRD pattern of the crushed crystals collected at room temperature. (b) The XRD pattern of an as-grown single crystal. The insets show the images and Laue spots. (c) The EDS spectrum of the crystal.

to verify the quality of as-grown crystals, we present the Rietveld-refined XRD pattern of the crushed crystals, as shown in Fig. 2(a). The refined structure of Cu_3TeO_6 fits the centrosymmetric $Ia-3$ cubic space group with unit cell parameters $a = b = c = 9.57336 \text{ \AA}$, in agreement with that previously reported [22], implying that the high structure quality of as-grown single crystals is confirmed. In addition, Fig. 2(b) presents the high-resolution scanned XRD pattern onto one naturally developed plane, which shows very sharp diffraction peaks well indexed by the $(h00)$ reflections. The three orthogonal directions calibrated as $x//[100]$, $y//[010]$, and $z//[001]$ were carefully determined by an analysis based on the consistency between the Laue diffraction spots and the XRD patterns, and the quadrate diffraction spots from each plane were observed in the inset of Fig. 2(b), consistent with the cubic lattice structure at room temperature. One unit cell

in this insulating tricopper tellurate Cu_3TeO_6 consists of eight regular TeO_6 octahedra and 24 copper ions [21].

Then, three well-oriented samples were cut into a rectangular parallelepiped shape, and are also presented in the inset of Fig. 2(b). Moreover, in Fig. 2(c), the chemical composition of these crystals was checked using the EDS technique, and the data show that the atomic ratio $\text{Cu}:\text{Te} = 36.9:12.2 = 3.02$, much close to the nominal ratio 3. This good stoichiometry is favored for a relatively reliable measurement of the electric and magnetic properties. Subsequently, the high-quality crystals were submitted to the magnetic and electric measurements.

B. Magnetic property

Figures 3(a)–3(c) show the measured dc magnetic susceptibility $\chi(T)$ in the T range from 10 K to 300 K under a measuring $H = 0.1 \text{ T}$ applied along the three orthogonal directions, respectively. The $\chi(T)$ curves along the $x//a$ -axis, $y//b$ -axis, and $z//c$ -axis exhibit typical the λ -shape anomaly feature at $T = T_N \sim 61 \text{ K}$, indicating the formation of a long-range AFM order, as seen from all three different directions. Earlier reports on Cu_3TeO_6 revealed a three-dimensional AFM order with collinear moments along the $[111]$ direction below T_N [23], well consistent with our results that there is only relatively weak magnetic anisotropy.

For more quantitative evaluation of possible magnetocrystalline anisotropy, the data along the three main axes are replotted into the T -dependent $\chi^{-1}(T)$ curves as well, shown in Figs. 3(d)–3(f), respectively. The Curie-Weiss fitting of the data above $T = 200 \text{ K}$ gives the Curie-Weiss temperature (θ_{CW}) in the $H//a$, $H//b$, and $H//c$ geometries as $\theta_{\text{CW}} \sim -138 \text{ K}$, -114 K , and -139 K , respectively, confirming the AFM exchange interactions of Cu^{2+} spins. The frustration factor defined as $f = |\theta_{\text{CW}}|/T_N \sim 2$ suggests a weak spin frustration in this compound.

M as a function of H was also measured in the geometry of H applied along the x , y , and z directions, shown in Figs. 3(g)–3(i). The $M(H)$ curves display a typical linear behavior and the absence of any magnetic transition with H up to 8 T. It is noted that Cu_3TeO_6 with a cubic lattice structure presents a slight magnetic anisotropy in Figs. 3(g)–3(i); however, it deserves to be given magnetic isotropy under the ground state along three axes. In fact, the magnetic anisotropy may come from the symmetry breaking due to the anisotropic Heisenberg antiferromagnetic interactions with multiple spin domains [26]. In addition, the value of magnetization under H up to 8 T is far less than the saturated magnetic moment $M_{\text{sat}} \sim 5.19 \mu_{\text{B}}/\text{f.u.}$ assuming that the Cu^{2+} spins have a moment of $S = 1/2$. Certainly, the high field magnetic measurement is highly deserved to reveal the spin dynamics in Cu_3TeO_6 , which is beyond the scope of this work and unfortunately not accessible at this moment.

C. Magnetoelectric effect

To explore the ME effect in the AFM phase, a comprehensive study of the T dependence of electric polarization along the $P//x$ (P_x), $P//y$ (P_y), and $P//z$ (P_z) directions under different H orientations was carefully conducted, and the data

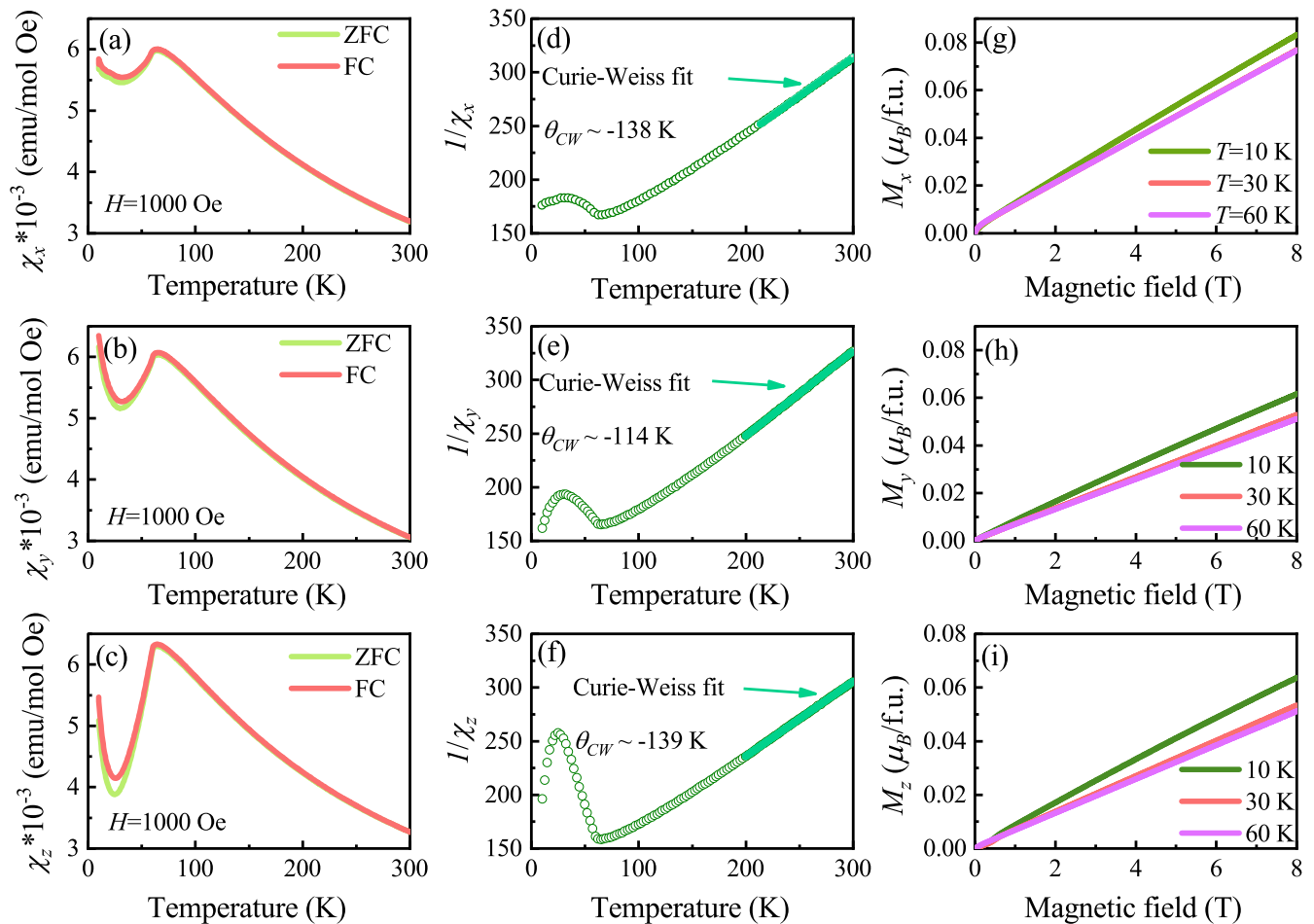


FIG. 3. (a)–(c) The T dependence of magnetic susceptibility (χ) of Cu_3TeO_6 under ZFC and FC modes measured at $H = 1000$ Oe in the x , y , and z directions, respectively. (d)–(f) The Curie-Weiss fitting χ^{-1} along three different directions. (g)–(i) H dependence of M measured at selected T in three different directions.

are summarized in Fig. 4. The results evidently reveal the intriguing ME tensor with nine nonzero components, a surprising consequence that deserves a more detailed discussion. It is seen that the data in the nine plots are presented with the identical P window, from $-25 \mu\text{C}/\text{m}^2$ to $25 \mu\text{C}/\text{m}^2$, so that the magnitudes of the ME responses can be compared quantitatively.

Imposed by the cubic space group, no spontaneous electric polarization is, in principle, allowed. Indeed, the magnetic point group $-3'$ allows the conjugation of nonzero components, but this issue will be discussed later. In general, the measured results well support the symmetry consideration. At zero magnetic field, there is an absence of ferroelectricity along the x , y , and z directions, while a polarization as large as $\sim 19 \mu\text{C}/\text{m}^2$, $\sim 17 \mu\text{C}/\text{m}^2$, and $\sim 16 \mu\text{C}/\text{m}^2$ is generated for P_x , P_y , and P_z at $H//z$, $H//x$, and $H//y$, respectively, under the presence of H up to 8 T. Moreover, the electric polarization can be fully reversed by applying a negative pooling field E , as shown in Figs. 4(c), 4(d), and 4(h) separately. More specifically, we present the T dependence of pyroelectric current I_x , I_y , and I_z under various H in the inset of Fig. 4, which exhibits a sharp peak near T_N , implying the magnetically induced ferroelectricity. Considering the cases of P_x ($H//x$) and P_x

($H//y$) in Figs. 4(a) and 4(b), respectively, one can see that P_x uncover an obvious linear ME behavior with $H//z$, while P_x are much weak under $H//x$ and $H//y$. Similar behaviors are observed in the other two cases, in which only two components, P_y ($H//x$) and P_z ($H//y$), are prominent. Thus, our data demonstrate a remarkable anisotropic ME effect in Cu_3TeO_6 .

Figures 5(a)–5(c) shows the field-induced electric polarization ΔP_x , ΔP_y , and ΔP_z as a function of H under $H//z$, $H//x$, and $H//y$, respectively, at selected T , and more intuitive linear ME effects are unambiguously presented. Taking $\Delta P_x(H//z)$ as an example, ΔP_x linearly increases to $\sim 18 \mu\text{C}/\text{m}^2$ with H up to 8 T at $T = 10$ K without saturation. In addition, ΔP_x can be fully reversed by changing the pooling E from $+E$ to $-E$, which indicates that Cu_3TeO_6 is magnetoelectric linearly in this AFM phase. Quite similar ME responses are observed in $\Delta P_y(H//x)$ and $\Delta P_z(H//y)$ cases, with the linear ME coefficients $\alpha_{xz} \approx \alpha_{yx} \approx \alpha_{zy} = 3.1 \text{ ps}/\text{m}$.

To explore the magnetically driven ferroelectricity in this PT symmetry system further, for reference we plot again the $M(H)$ curves with H varying from -8 T to $+8$ T, as shown in Figs. 5(d)–5(f). It is clearly seen that the independent ferroic order P and M are always perpendicular to each other, and six ME states—namely, $(\pm P_x, \pm M_z)$, $(\pm P_y, \pm M_x)$, and

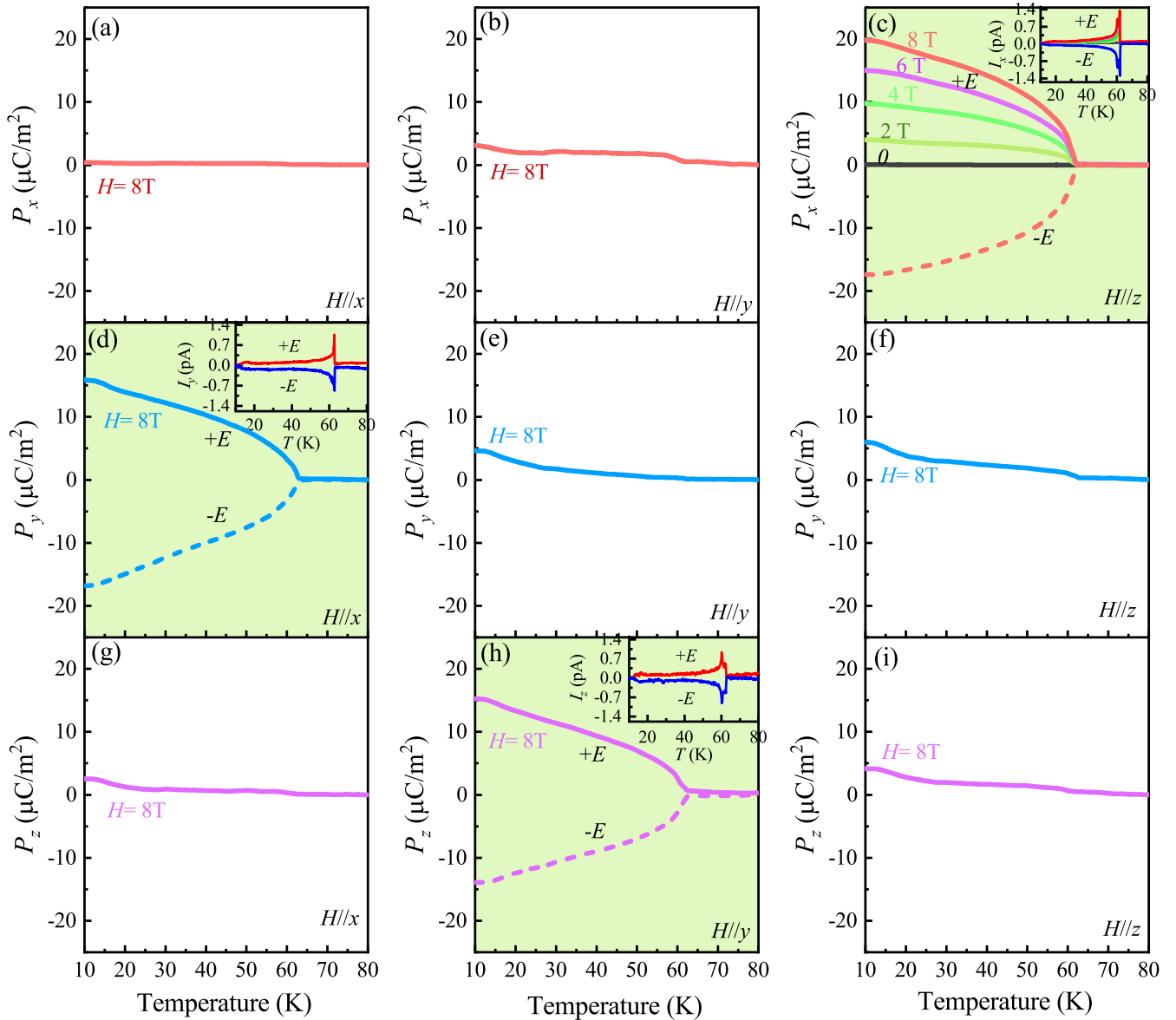


FIG. 4. The T dependence of P_x , P_y , and P_z under orthogonal H along (a)–(c) the x direction, (d)–(f) the y direction, and (g)–(i) the z direction, respectively. The insets show the T dependence of pyroelectric current I_x , I_y , and I_z in the magnetic field and pooling electric field ($\pm E$) along the z , x , and y directions.

($\pm P_z$, $\pm M_y$)—can be preserved by selection of H in a specific direction, as shown in Fig. 6(a), noting that the other components are much more weak and are negligible here. Hence, such interesting coupling effect makes Cu_3TeO_6 a very appealing prototype for crystals in the $A_3\text{TeO}_6$ ($A = \text{Mn}, \text{Ni}, \text{Cu}, \text{Co}$) family in multifunctional applications [27–29]. In addition, the existence of off-diagonal components in the ME tensor may imply the occurrence of the ferrotoroidal order in Cu_3TeO_6 , calling for future theoretical and experimental investigations, e.g., second harmonic generation spectroscopy. Due to the isotropic feature of the spin order, both M and P may theoretically rotate freely within the three-dimensional space, allowing the formation of single ME domains. However, it is suggested that the ME pooling procedure in our measurement is not sufficient to obtain single ME domains in which anisotropic ME responses are found, consistent with

a previous report, e.g., $\text{LaMn}_3\text{Cr}_4\text{O}_{12}$ and hexagonal ferrite [14,30].

D. Magnetoelectric tensor analysis

Subsequently, let us discuss the ME coupling effect based on magnetic point group analysis, which allows one to predict the appearance of electric polarization. It is well known that distinctive magnetic structures combining with crystallographic lattices may give rise to a ME effect in low-energy excited states. Materials with these features are strictly limited by the magnetic point group. As presented earlier, Cu_3TeO_6 exhibits a linear ME response in three orthogonal directions. Then, the ME tensor coefficients in Cartesian xyz coordinates can be checked as follows. Generally, the H -induced first-rank tensor P_i [A s/m^2] is linearly proportional to the applied first

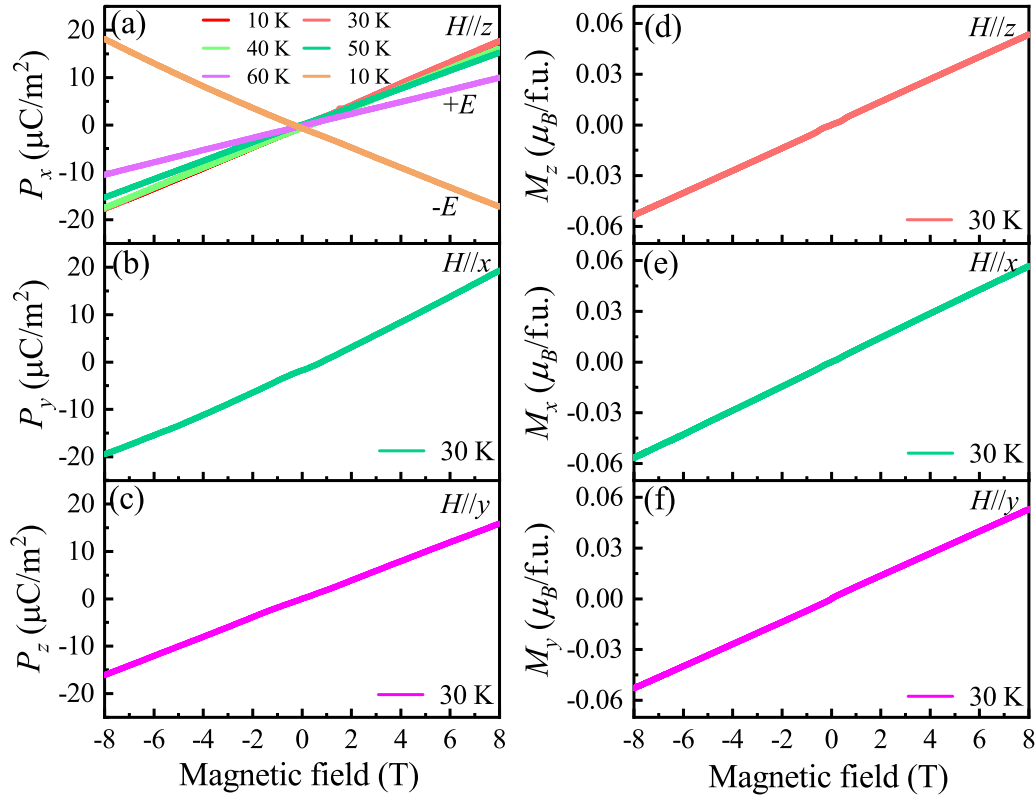


FIG. 5. The H dependence of P_x , P_y , and P_z under H along the (a) z , (b) x , and (c) y directions at selected T , respectively. (d)–(f) The H dependence of M_z , M_x , and M_y , respectively.

rank tensor H_j [A/m] through the second-rank tensor ME coefficients α_{ij} [s/m] ($P_i = \alpha_{ij}H_j = \pm t_{ik}\alpha_{kl}t'_{lj}H_j$), where the t is transformation matrix. The generating elements are a three-fold central inversion plus time reversal axis ($-3'$)/[111] direction. According to Neumann's principle [31], the matrix is transformed as

$$\begin{aligned}
 \begin{pmatrix} \alpha'_{11} & \alpha'_{12} & \alpha'_{13} \\ \alpha'_{21} & \alpha'_{22} & \alpha'_{23} \\ \alpha'_{31} & \alpha'_{32} & \alpha'_{33} \end{pmatrix} &= (-1)(-1) \begin{pmatrix} 0 & 1 & 0 \\ 0 & 0 & 1 \\ 1 & 0 & 0 \end{pmatrix} \\
 &\times \begin{pmatrix} \alpha_{11} & \alpha_{12} & \alpha_{13} \\ \alpha_{21} & \alpha_{22} & \alpha_{23} \\ \alpha_{31} & \alpha_{32} & \alpha_{33} \end{pmatrix} \begin{pmatrix} 0 & 0 & 1 \\ 1 & 0 & 0 \\ 0 & 1 & 0 \end{pmatrix} \\
 &= \begin{pmatrix} \alpha_{22} & \alpha_{23} & \alpha_{21} \\ \alpha_{32} & \alpha_{33} & \alpha_{31} \\ \alpha_{12} & \alpha_{13} & \alpha_{11} \end{pmatrix} \\
 &= \begin{pmatrix} \alpha_{11} & \alpha_{12} & \alpha_{13} \\ \alpha_{21} & \alpha_{22} & \alpha_{23} \\ \alpha_{31} & \alpha_{32} & \alpha_{33} \end{pmatrix}, \quad (1)
 \end{aligned}$$

which can be satisfied only if $\alpha_{11} = \alpha_{22} = \alpha_{33}$, $\alpha_{12} = \alpha_{23} = \alpha_{31}$, and $\alpha_{13} = \alpha_{21} = \alpha_{32}$. Therefore, the ME matrix for the magnetic point group $-3'$ in xyz coordinates is

$$\alpha_{ij} = \begin{pmatrix} \alpha_{11} & \alpha_{12} & \alpha_{13} \\ \alpha_{13} & \alpha_{11} & \alpha_{12} \\ \alpha_{12} & \alpha_{13} & \alpha_{11} \end{pmatrix}, \quad (2)$$

where all nine coefficients can be nonzero. The ME coupling coefficients defined by dP/dH $\alpha_{13} = \alpha_{21} = \alpha_{32} = 3.1$ ps/m

are obtained according to our experimental results. Nevertheless, the other components in this ME coupling tensor exhibit weak magnitude, which may be attributed to the suppressed ME domains. Therefore, SOS in relation to broken symmetries is very powerful to predict new materials with magnetism-driven ferroelectricity and a linear ME effect [16]. For instance, materials with specific magnetic point groups, including $-1'$, $-3'$, $-4'$, $-6'$, and so on, may serve as potential candidates for new magnetoelectrics.

Next, we discuss the possible microscopic mechanism of the ME coupling effect in Cu_3TeO_6 . As there are many magnetic ions in a single magnetic unit cell, for simplicity, we only consider three pair of Cu^{2+} moments with center inversion symmetry, as shown in Fig. 6(b). Previous neutron scattering suggests two possible magnetic configurations: (i) the collinear AFM order and (ii) the noncollinear configuration [23]. While the collinear case is considered appropriately [21,22], each up-spin (S_1) paralleling [111] relates to a down-spin (S_2) antiparallel to [111] by the center point $-3'$ central inversion, belonging to a magnetic group with PT symmetry. Obviously, in this AFM ground state, there is no spontaneous P and net M due to the centrosymmetric structure. When H is applied parallel to the S_1 moment ($m_{//}$ direction), a simple and conceptually important model, in which the S_1 moment parallel to the $m_{//}$ direction tends to increase while the antiparallel moment S_2 decreases, can be constructed, as shown in Fig. 6(b), implying that the simultaneous breaking of both time reversal symmetry and spatial inversion symmetry exhibits the ME effect. Similarly, with H_{\perp} (m_{\perp} direction), all the moments tend to tilt a little bit to H , and thus the

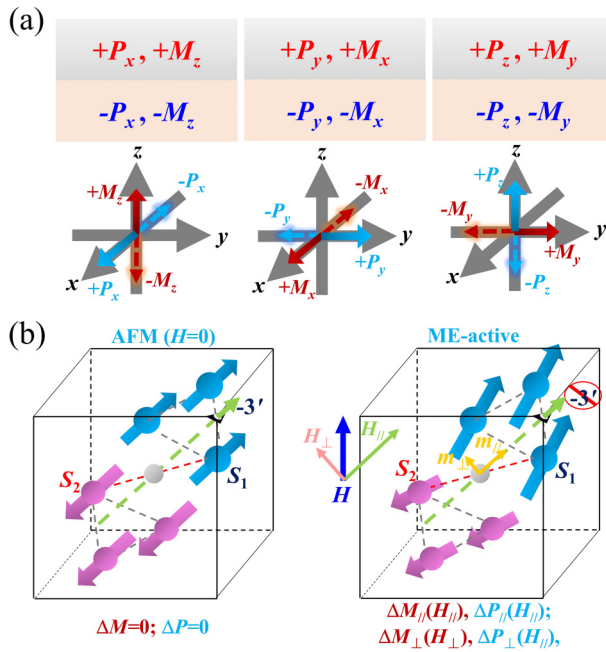


FIG. 6. (a) A schematic illustration of the relationship between electric polarization and magnetization under external magnetic field. Six ME states—namely, $(\pm P_x, \pm M_z)$, $(\pm P_y, \pm M_x)$, and $(\pm P_z, \pm M_y)$ —are presented. (b) The adjacent three pairs of spins with magnetic point group $-3'$. The light-blue and magenta arrows denote the spins of paralleling and antiparalleling to threefold axis, respectively. Electric polarization ΔP is induced through the exchange striction mechanism and the DM interaction simultaneously. The light-yellow arrows are used to indicate net magnetization and local electric dipole moments of H driven.

H -induced ferromagnetic interaction also breaks the threefold rotation symmetry. One can see that the exchange striction associated with symmetric superexchange shortens the bonds between the parallel spins. Consequently, the linear magnetic

ordering breaks $-3'$ inversion symmetry on magnetic sites and induces a local electric dipole moment by the scalar product of the pair magnetic moments, denoted as $p \propto (S_{1i} \cdot S_{2j})$. Therefore, a net electric polarization ΔP perpendicular to H , concomitant with a net magnetization along the H direction, can be obtained. While the ferromagnetic interaction induces net electric polarization perpendicular to H through the Dzyaloshinskii-Mariya (DM) interaction [32]. Of course, the appearance of a noncollinear spin order implies that the DM interaction may also contribute to the ferroelectricity in Cu_3TeO_6 [33], calling for further theoretical investigation.

IV. CONCLUSION

In conclusion, we have investigated the distinctive magnetoelectric effect in the Dirac magnon material Cu_3TeO_6 with a highly symmetric cubic phase. The results reveal nine nonvanished components of the ME tensor, while only P_x ($H//z$), P_y ($H//x$), and P_z ($H//y$) display a remarkable linear response to H . In particular, we observe six ME states—namely, $(\pm P_x, \pm M_z)$, $(\pm P_y, \pm M_x)$, and $(\pm P_z, \pm M_y)$ —that can be generated by an external magnetic field in a specific direction, which makes Cu_3TeO_6 a very appealing prototype for multifunctional applications. The existence of off-diagonal components in the ME tensor may imply the occurrence of the ferrotoroidal order in Cu_3TeO_6 , calling for future theoretical and experimental investigations. Our results point toward Cu_3TeO_6 as a new, linear ME material and may provide a platform on which distinctive ME responses in the presence of topological properties can be explored.

ACKNOWLEDGMENT

This work was financially supported by the National Natural Science Foundation of China (Grants No. 92163210, No. 11874031, No. 12274231, No. 11834002, No. 11947092, No. 12074111, No. 51721001, and No. 11974167).

- [1] Y. Tokura, S. Seki, and N. Nagaosa, Multiferroics of spin origin, *Rep. Prog. Phys.* **77**, 076501 (2014).
- [2] M. Fiebig, Revival of the magnetoelectric effect, *J. Phys. D: Appl. Phys.* **38**, R123 (2005).
- [3] N. A. Spaldin and R. Ramesh, Advances in magnetoelectric multiferroics, *Nat. Mater.* **18**, 203 (2019).
- [4] S.-W. Cheong and M. Mostovoy, Multiferroics: A magnetic twist for ferroelectricity, *Nat. Mater.* **6**, 13 (2007).
- [5] S. Dong, J.-M. Liu, S.-W. Cheong, and Z. Ren, Multiferroic materials and magnetoelectric physics: Symmetry, entanglement, excitation, and topology, *Adv. Phys.* **64**, 519 (2015).
- [6] Y. J. Choi, H. T. Yi, S. Lee, Q. Huang, V. Kiryukhin, and S.-W. Cheong, Ferroelectricity in an Ising Chain Magnet, *Phys. Rev. Lett.* **100**, 047601 (2008).
- [7] T. Kimura, T. Goto, H. Shintani, K. Ishizaka, T. Arima, and Y. Tokura, Magnetic control of ferroelectric polarization, *Nature (London)* **426**, 55 (2003).
- [8] N. Hur, S. Park, P. A. Sharma, J. S. Ahn, S. Guha, and S.-W. Cheong, Electric polarization reversal and memory in a multi-ferroic material induced by magnetic fields, *Nature (London)* **429**, 392 (2004).
- [9] G. Q. Zhang, S. Dong, Z. B. Yan, Y. Y. Guo, Q. F. Zhang, S. Yunoki, E. Dagotto, and J.-M. Liu, Multiferroic properties of $\text{CaMn}_7\text{O}_{12}$, *Phys. Rev. B* **84**, 174413 (2011).
- [10] T. Kurumaji, S. Ishiwata, and Y. Tokura, Doping-Tunable Ferromagnetic Phase with Large Linear Magnetoelectric Effect in a Polar Magnet $\text{Fe}_2\text{Mo}_3\text{O}_8$, *Phys. Rev. X* **5**, 031034 (2015).
- [11] Y. S. Tang, J. H. Zhang, L. Lin, R. Chen, J. F. Wang, S. H. Zheng, C. Li, Y. Y. Zhang, G. Z. Zhou, L. Huang, Z. B. Yan, X. M. Lu, D. Wu, X. K. Huang, X. P. Jiang, and J.-M. Liu, Metamagnetic transitions and magnetoelectricity in the spin-1 honeycomb antiferromagnet $\text{Ni}_2\text{Mo}_3\text{O}_8$, *Phys. Rev. B* **103**, 014112 (2021).
- [12] Y. Kitagawa, Y. Hiroka, T. Honda, T. Ishikura, H. Nakamura, and T. Kimura, Low-field magnetoelectric effect at room temperature, *Nat. Mater.* **9**, 797 (2010).
- [13] X. Wang, Y. S. Chai, L. Zhou, H. B. Cao, C.-D. Cruz, J. Y. Yang, J. H. Dai, Y. Y. Yin, Z. Yuan, S. J. Zhang, R. Z. Yu,

- M. Azuma, and Y. Shimakawa, Observation of Magnetoelectric Multiferroicity in a Cubic Perovskite System: $\text{LaMn}_3\text{Cr}_4\text{O}_{12}$, *Phys. Rev. Lett.* **115**, 087601 (2015).
- [14] S. Seki, S. Ishiwata, and Y. Tokura, Magnetoelectric nature of skyrmions in a chiral magnetic insulator Cu_2OSeO_3 , *Phys. Rev. B* **86**, 060403(R) (2012).
- [15] L. Weymann, L. Bergen, Th. Kain, A. Pimenov, A. Shuvaev, E. Constable, D. Szaller, B. V. Mill, A. M. Kuzmenko, V. Yu. Ivanov, N. V. Kostyuchenko, A. I. Popov, A. K. Zvezdin, A. Pimenov, A. A. Mukhin, and M. Mostovoy, Unusual magnetoelectric effect in paramagnetic rare-earth langasite, *npj Quantum Mater.* **5**, 61 (2020).
- [16] S.-W. Cheong, SOS: Symmetry-operational similarity, *npj Quantum Mater.* **4**, 53 (2019).
- [17] L. Ding, X. H. Xu, H. O. Jeschke, X. J. Bai, E. X. Feng, A. S. Alemanyeh, J. Kim, F.-T. Huang, Q. Zhang, X. X. Ding, N. Harrison, V. Zapf, D. Khomskii, I. I. Mazin, S.-W. Cheong, and B. H. Cao, Field-tunable toroidal moment in a chiral-lattice magnet, *Nat. Commun.* **12**, 5339 (2021).
- [18] S. Seki, X. Z. Yu, S. Ishiwata, and Y. Tokura, Observation of skyrmions in a multiferroic material, *Science* **336**, 198 (2012).
- [19] D. M. Burn, R. Brearton, K. J. Ran, S. L. Zhang, G. van der Laan, and T. Hesjedal, Periodically modulated skyrmion strings in Cu_2OSeO_3 , *npj Quantum Mater.* **6**, 73 (2021).
- [20] Y. Tokura, M. Kawasaki, and N. Nagaosa, Emergent functions of quantum materials, *Nat. Phys.* **13**, 1056 (2017).
- [21] W. L. Yao, C. Y. Li, L. C. Wang, S. J. Xue, Y. Dan, K. Lida, K. Kamazawa, K. K. Li, C. Fang, and Y. Li, Topological spin excitations in a three-dimensional antiferromagnet, *Nat. Phys.* **14**, 1011 (2018).
- [22] S. Bao, J. H. Wang, W. Wang, Z. W. Cai, S. C. Li, Z. Ma, D. Wang, K. J. Ran, Z.-Y. Dong, D. L. Abernathy, S.-L. Yu, X. G. Wan, J.-X. Li, and J. S. Wen, Discovery of coexisting Dirac and triply degenerate magnons in a three-dimensional antiferromagnet, *Nat. Commun.* **9**, 2591 (2018).
- [23] M. Herak, H. Berger, M. Prester, M. Miljak, I. Zivkovic, O. Milat, D. Drobac, S. Popovic, and O. Zaharko, Novel spin lattice in Cu_3TeO_6 : An antiferromagnetic order and domain dynamics, *J. Phys.: Condens. Matter* **17**, 7667 (2005).
- [24] Z. Z. He and M. Itoh, Magnetic behaviors of Cu_3TeO_6 with multiple spin lattices, *J. Magn. Magn. Mater.* **354**, 146 (2014).
- [25] L. Lin, H. X. Zhu, X. M. Jiang, K. F. Wang, S. Dong, Z. B. Yan, Z. R. Yang, J. G. Wan, and J.-M. Liu, Coupling ferroelectric polarization and magnetization in spinel FeCr_2S_4 , *Sci. Rep.* **4**, 6530 (2014).
- [26] M. Herak, Cubic magnetic anisotropy of the antiferromagnetically ordered Cu_3TeO_6 , *Solid State Commun.* **151**, 1588 (2011).
- [27] J. Kim, J. Yang, C. J. Won, K. Kim, B. Kim, D. Obeysekera, D. W. Lee, and S.-W. Cheong, Helical versus collinear antiferromagnetic order tuned by magnetic anisotropy in polar and chiral $(\text{Ni}, \text{Mn})_3\text{TeO}_6$, *Phys. Rev. Mater.* **5**, 094405 (2021).
- [28] J. W. Kim, S. Artyukhin, E. D. Mun, M. Jaime, N. Harrison, A. Hansen, J. J. Yang, Y. S. Oh, D. Vanderbilt, V. S. Zapf, and S.-W. Cheong, Successive Magnetic-Field-Induced Transition and Colossal Magnetoelectric Effect in Ni_3TeO_6 , *Phys. Rev. Lett.* **115**, 137201 (2015).
- [29] M. Hudl, R. Mathieu, S. A. Ivanov, M. Weil, V. Carolus, T. Lottermoser, M. Fiebig, Y. Tokunaga, Y. Taguchi, Y. Tokura, and P. Nordblad, Complex magnetism and magnetic-field-driven electrical polarization of Co_3TeO_6 , *Phys. Rev. B* **84**, 180404(R) (2011).
- [30] V. Kocsis, T. Nakajima, M. Matsuda, A. Kikkawa, Y. Kaneko, J. Takashima, K. Kakurai, T. Arima, Y. Tokunaga, Y. Tokura, and Y. Taguchi, Stability of multiferroic phase and magnetization-polarization coupling in Y-type hexaferrite crystals, *Phys. Rev. B* **101**, 075136 (2020).
- [31] R. E. Newnham, *Properties of Materials: Anisotropy, Symmetry, Structure* (Oxford University Press, Oxford, 2005).
- [32] L. C. Chapon, P. G. Radaelli, G. R. Blake, S. Park, and S.-W. Cheong, Ferroelectricity Induced by Acentric Spin-Density Waves in YMn_2O_5 , *Phys. Rev. Lett.* **96**, 097601 (2006).
- [33] H. Katsura, N. Nagaosa, and A. V. Balatsky, Spin Current and Magnetoelectric Effect in Noncollinear Magnets, *Phys. Rev. Lett.* **95**, 057205 (2005).